

## A Fracture Mechanics-Based Approach to Simulate Die Pick-up Process

Sandeep Shantaram, Ph.D., Yi Hsuan Tsai, Yao Jung Chang  
NXP Semiconductors Inc.  
TX, USA  
sandeep.shantaram@NXP.com

### ABSTRACT

Integrated circuit die pick-up event is an important process step in advanced packages such as wafer level chip scale packages (WLCSP). The productivity is sensitive to 3 primary factors which include die-crack risk due to ejection process, die knocking to the neighboring dies, unsuccessful delamination of the chip-on-substrate structure. This paper provides a procedure to simulate die pick-up process based on contact-debonding fracture mechanics approach. Also, ejection height predicted by the model will be compared with the empirical findings for various needle configuration. Finally, needle selection rule for WLCSP family will be provided.

Key words: die pick-up process, WLCSP, FEM, Contact-debonding.

### INTRODUCTION

Wafer Level Chip Scale Package (WLCSP) refers to the technology of packaging an integrated circuit at the wafer level have been extensively used in the semiconductor industry due to their multiple benefits which includes reduced package size, enhanced thermal conduction characteristic with die-to-PCB inductance minimized. On the other hand WLCSP pose challenges during the electronic assembly. And one such challenge includes handling thin semiconductor silicon dies during the die pick up process assembly step (Peng et.al, Liu et.al, Xu et.al). Figure 1 shows one of the common failure modes encountered during the die pickup assembly process step which is a die-brittle crack in the side wall due to knocking to the neighboring die. And other two less common failure modes includes die brittle crack due to over-stress exerted by ejection needle and unsuccessful pickup due to improper ejection height setting in combination with needle/s configuration.

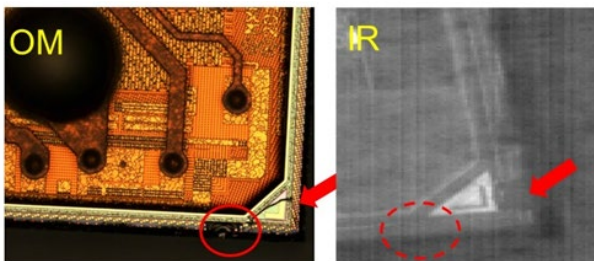


**Figure 1.** Die brittle crack due to knocking, a common failure mode during die-pick up assembly process step  
Figure 2 shows the schematic of WLCSP die pick up set-up.

Figure 3, shows various applied forces/pressure present during the die pickup assembly process step. In the Figure 4, step-by-step die pick-up and eject process is being described. In the first step, the pickup head with rubber tip starts to move down and touch on device top surface with unit touching pressure. The second step, the needle raises up synchronously with rubber tip to push up the die, the dicing tape starts to peel off from the die due to downward vacuum pressure under the tape, when the tape contact area become very small then the die will be picked up successfully by rubber tip with vacuum suction. The step 2 is the most critical part for product quality and process productivity due to substrate suffers various force during upward motion.

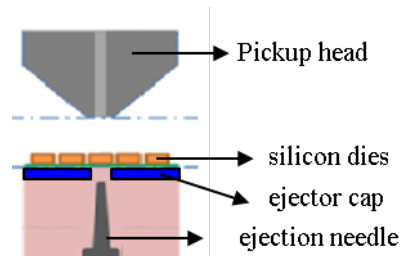


**Figure 2.** Schematic of die pick up & eject tool set-up

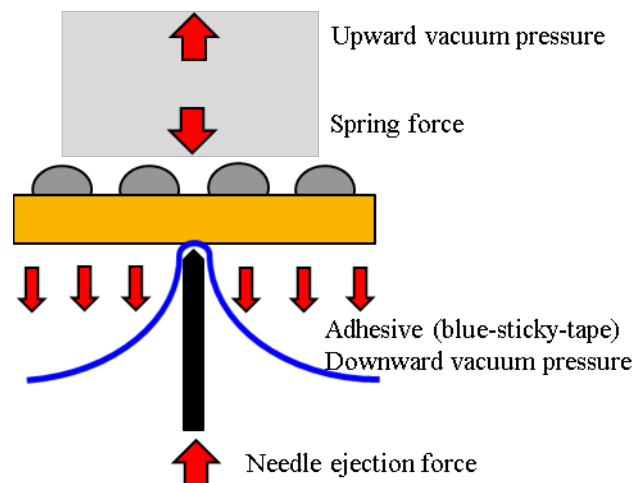


**Figure 3.** Various applied forces/pressure present during the die pickup assembly step

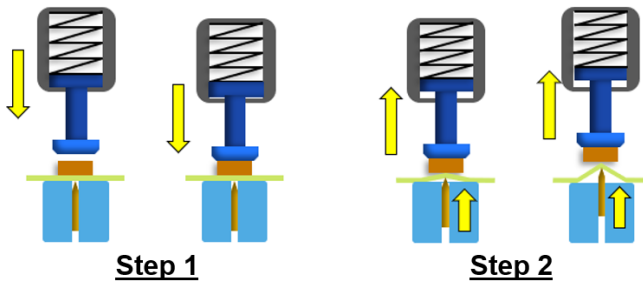


Figure 4. Die pickup and eject assembly process steps

## EXPERIMENTAL SETUP

### Design of Experiments and Test Results

In order to analyze the chip peeling behavior in actual application condition, the empirical test uses dummy silicon wafers which are mounted on a dicing tape for test, the die size is  $3.36 \times 3.55 \text{ mm}^2$  with silicon thickness  $175\mu\text{m} + 25\mu\text{m}$  BSP total of  $200\mu\text{m}$ , all the test wafers underwent similar grinding and sawing process to avoid discrepancy in test results due to manufacturing processes, and then they are subjected to pick and place process in chip sorter machine for data collection. Total 4 needle pitch conditions have been selected for test including single needle in the center, 4 needles with 1mm needle pitch, 4 needles with 1.5mm needle pitch, 4 needles with 2mm needle pitch to verify the relation between needle layout and die pickup results (see Figure 5). For each needle pitch conditions, tested 5 samples to check the repeatability and to isolated the failure modes including die-crack, die-to-die knocking, unsuccessful delamination of the chip-on-substrate structure.

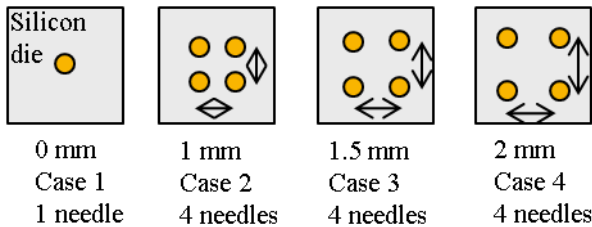


Figure 5. needle locations for various design cells w.r.t silicon die (note: images not scaled)

In the die-pickup process, die is successfully picked when ~100% tape peeling off takes place. Therefore tape peeling is a reliable indicator to predict the pickup fail results. Table 1, provides the results for the controlled die-pickup test. From the test results it is clear that the single center needle has least ejection height for successful pick up since needle configuration makes tape peeling from die edge easier to start and propagate steady. On the other hand, all the 4 needle configuration cases show relatively higher ejection height for successful pick this is due to additional constraints introduced by the all 4 needles when it in contact with the dicing tape. Also, needle pitch has an influence on ejection height in the 4 needle cases. The smallest pitch tested which is 1mm shows the highest ejection this is due to the constrains from 4 needles which are comparatively closer to each other which

significantly restricts the relative movements of the tape with in the area of the 4 needles.

Table 1. Test results for various needle configuration

cases	Needle layout and pitch	Ejection height of initial tape peeling	Ejection height of die fully picked up
1	single center needle	90 $\mu\text{m}$	170 $\mu\text{m}$
2	4 pins w/ 1mm pitch	230 $\mu\text{m}$	370 $\mu\text{m}$
3	4 pins w/ 1.5mm pitch	170 $\mu\text{m}$	310 $\mu\text{m}$
4	4 pins w/ 2mm pitch	150 $\mu\text{m}$	250 $\mu\text{m}$

Figure 6, shows the typical delamination initiation and growth of die-to-dicing tape. Typical needle ejection results show that tape peeling start from the edge of the die and propagate into the die center

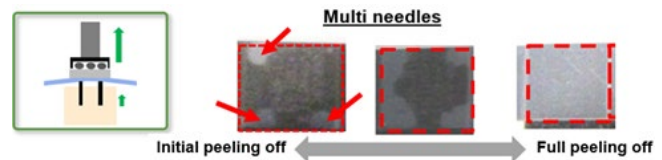


Figure 6. die-to-dicing tape interface delamination for a typical 4 needle case.

## MATERIAL CHARACTERIZATION

### Blue-Dicing tape material characterization

In this study, prior to the interface material characterization, the stand alone blue-dicing tape (base material is polyolefin) material have been characterized using tensile test setup (Figure 7). Sample size (length x width x thickness) of  $100\text{mm} \times 15\text{mm} \times 0.085 \text{ mm}$  is used. Tensile speed used in this study is  $200\text{mm}/\text{min}$ .

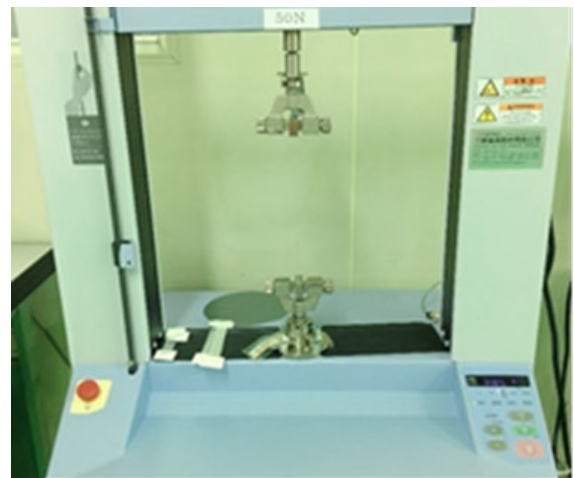
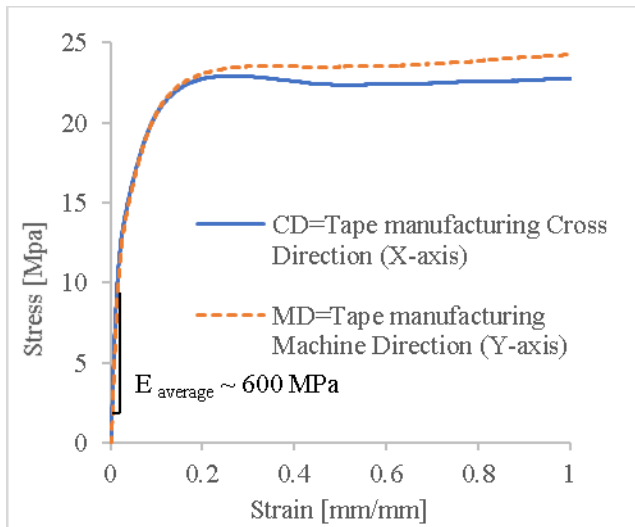


Figure 7. Tensile test setup



**Figure 8.** Stress-strain behavior of blue dicing tape under uniaxial tensile loading conditions

From the Figure 8, it is clear that the blue dicing tape has highly non-linear behavior. Therefore in order to implement this material type in a FE code hyper-elastic model will be required. Several forms of strain energy potentials describe the hyper-elasticity of materials. These are based on either strain invariants or principal stretches. The behavior of materials is assumed to be incompressible or nearly incompressible ( $\nu = 0.5$ ).

Two parameter Mooney-Rivlin Model is chosen in this study for simplicity and the corresponding form of the strain energy potential is:

$$W = c_{10}(\bar{I}_1 - 3) + c_{01}(\bar{I}_2 - 3) + \frac{1}{d^*}(J - 1)^2 \quad (1)$$

Where:  $W$  = strain energy potential;  $\bar{I}_1$  = first deviatoric strain invariant;  $\bar{I}_2$  = second deviatoric strain invariant;  $c_{10} = 100$  MPa,  $c_{01} = 0$  as material constants,  $d^*$  = material incompressibility parameter = set to  $0 \text{ Pa}^{-1}$ .

The physical meaning of parameters used in the Mooney-Rivlin model is described as,

Initial shear modulus

$$\mu = 2(c_{10} + c_{01}) \quad (2)$$

Initial bulk modulus

$$K = \frac{2}{d^*} \quad (3)$$

Where:

$$d^* = \left( \frac{1-2\nu}{c_{10}+c_{01}} \right) \quad (4)$$

### Measurement of Adhesion Strength

Adhesion measurements for the bi-material interface i.e., silicon with back-side-protection to the dicing tape (polyolefin) at room temperature were carried out using  $180^\circ$  peel test in a tensile tester. Figure 9a, shows the 2D schematic of  $180^\circ$  peel test (B. A., Moris) and Figure 9b shows the test set-up for the adhesion measurement with tensile tester. Test were carried out using ASTM standards D1876. Force and displacement data were recorded using data acquisition system for the multiple test samples. Figure 10, shows the test results of  $180^\circ$  peel test on 4 samples. Data indicates variation among the samples are minimal.

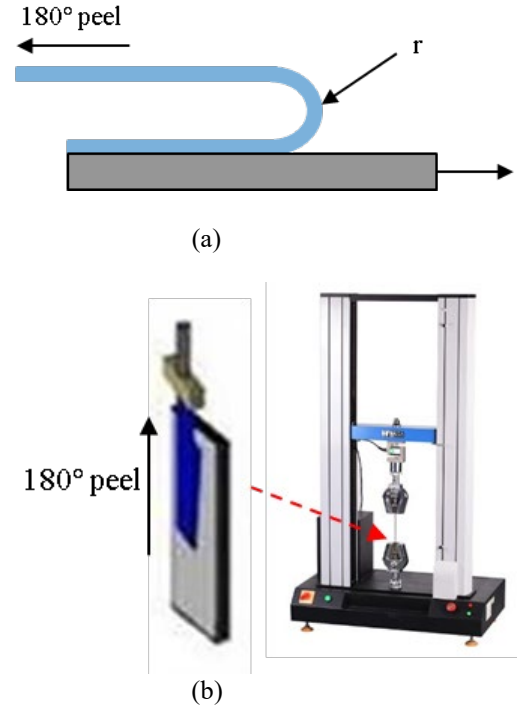


**Figure 9.** (a) 2D schematic of  $180^\circ$  peel test (b) Test set-up for adhesion measurement with tensile tester

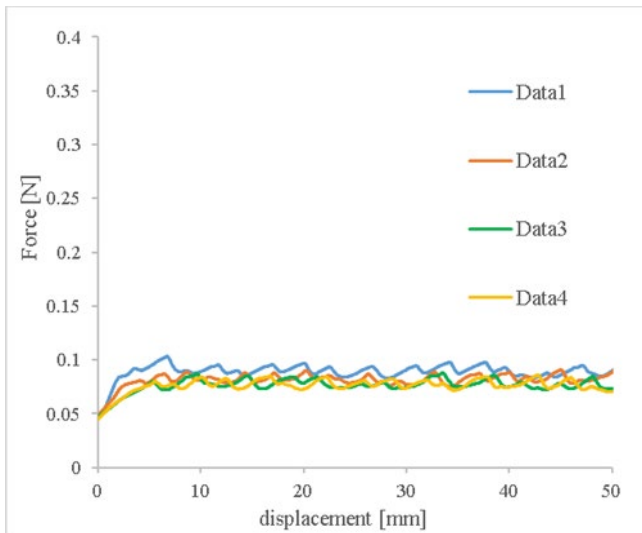


**Figure 10.** Force (N) vs. Displacement (mm) data for 4 test sample for 180° peel test

### Fracture Parameters for the Interface

Interfacial fracture parameters have been extracted using numerical analysis in conjunction with the 180° peel test data. In this study, as far as numerical analysis is concerned, interface delamination is modeled with the contact elements also referred as debonding. Debonding is modeled with contact elements which are bonded and have a cohesive zone material model defined. This debonding technique is easy to model since contact definition can be easily modified to include debonding, and standard contact and debonding can be simulated with the same contact definitions.

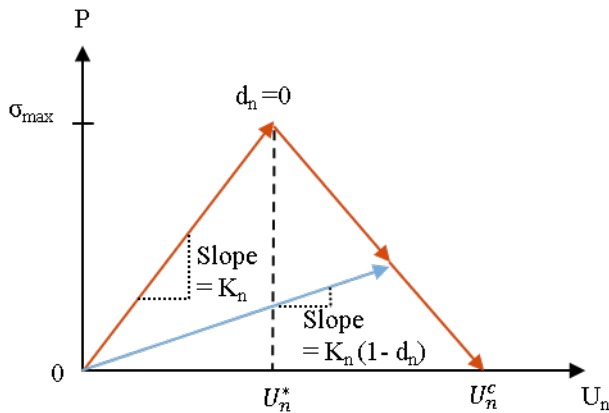


**Figure 11.** Bilinear traction-separation material behavior is used to define the normal failure properties

The cohesive zone material model with bilinear behavior is defined as:

$$\sigma_y = K_n U_y (1 - d) \quad (5)$$

$$\tau_x = K_t U_x (1 - d) \quad (6)$$

Where:  $\sigma_y$  = normal contact stress (tension) in y direction;  $\tau_x$  = tangential contact stress in x direction;  $K_n$  = normal contact stiffness,  $K_t$  = tangential contact stiffness,  $U_n$  = contact gap;  $U_y$  = contact slip distance in y direction;  $U_x$  = contact slip distance in x direction;  $d$  = debonding parameter

In this study, mixed mode failure is used. Figure 11, shows the bi-linear traction-separation plot which is used to define the normal failure (Mode-I) properties. A similar traction-separation plot is used to define the in-plane shear failure (Mode-II) properties <sup>not shown</sup>.

In this work, commercial finite element code is used to extract fracture parameters. Figure 12, shows the geometry details of 180° peel test simulation using 2D plane strain model with mesh details which uses quadratic shape function. Where silicon die and back side protection layers are modeled as linear-elastic behavior and dicing tape modeled as hyper-elastic behavior. Figure 13, provides the details of boundary and loading conditions assumed to reproduced 180-degree peel test results. The process of debonding and crack propagation is a nonlinear process. In the simulation settings, formulation is set to pure penalty type with large deflection turned ON.

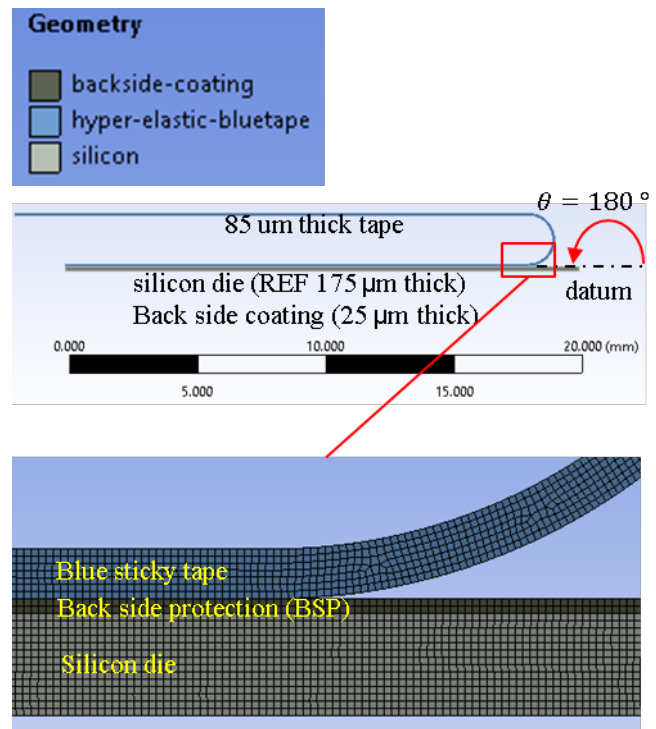


**Figure 12.** Geometry details of 180° peel test simulation using 2D plane strain analysis

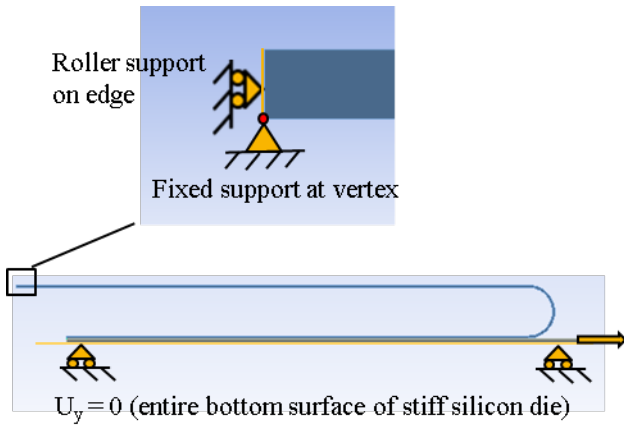
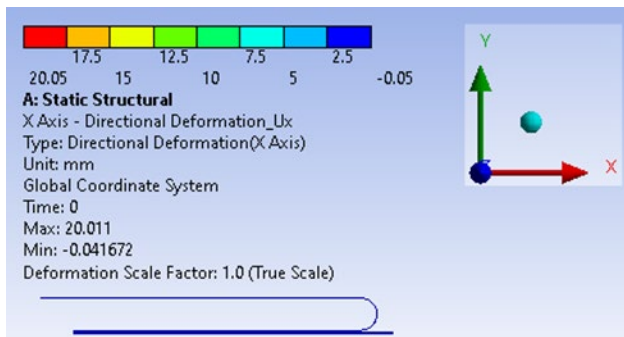
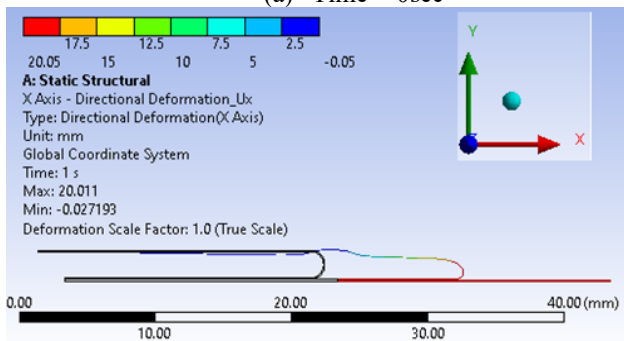


**Figure 13.** Boundary and loading conditions (25 °C)

Figure 14, shows the simulation results for the 180-degree peel test at various loading steps. Figure 15, shows the calibrated FE model with the trial and error scheme being implemented to extract the interface fracture parameters in order to fit the force-displacement experimental data. In the same figure, initial spike in the reaction force is due to relatively higher tape's radius of curvature assumption in the model to avoid any convergence issue. Also, Table 2 provides the finalized fracture parameter details which will be used to simulate die-pickup process.



(a) Time = 0sec



(b) Time > 0sec at  $U_x = 20$  mm

**Figure 14.** Simulation of 180 peel test to extract interfacial fracture parameters. (a) structure at rest  $t = 0$  sec, (b) structure subjected to axial displacement  $U_x = 20$  mm

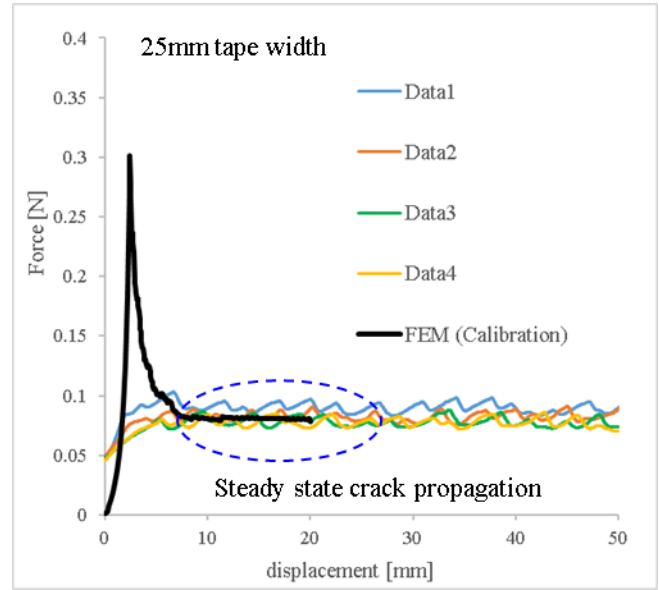


**Figure 15.** Calibration of force-displacement data by user defined interfacial fracture parameters

**Table 2.** Fracture Parameters

Property	Silicon die with backside coating (epoxy) to the blue-dicing tape (polyolefin)
Debonding interface mode	Mixed
Maximum normal contact stress	0.045 MPa
Critical fracture energy for normal separation	0.142 J/m <sup>2</sup>
Maximum equivalent tangential contact stress	0.045 MPa
Critical fracture energy for tangential separation	0.142 J/m <sup>2</sup>

### MODEL FLOW FOR DIE PICKUP PROCESS

The die pickup process has been simulated using 3D FEM approach with quarter symmetry assumption with single center die to reduce the computation burden. Also, simulation is carried out by assuming quasi-static loading conditions i.e., no inertial effects considered. Figure 16, provides the model geometry details. Silicon die, back-side polymer coating and stiff-needle modeled as linear-elastic behavior and the blue dicing tape modeled as hyper-elastic behavior whose properties have been described in the material characterization section. Needle tip dimensions of radius 80  $\mu$ m has been considered as per experimental setting.



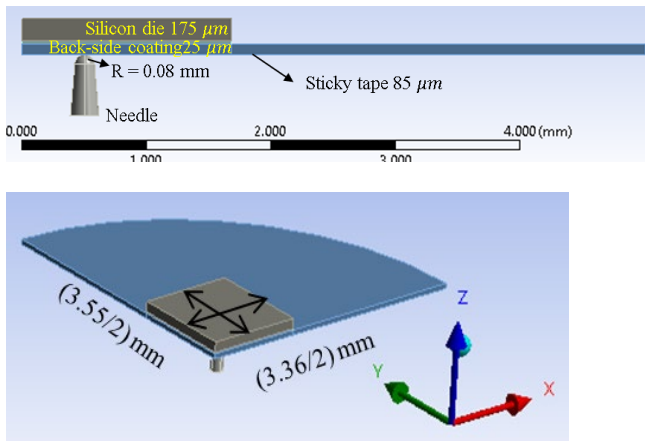


**Figure 16.** die-pickup 3D model geometry details for 4 needle 1 mm pitch case.

Following list provide the boundary and loading conditions:

1. Maximum vertical displacement of 600 μm applied to the bottom surface of the needle
2. 80 KPa of vacuum on sticky-tape's bottom surface
3. Total static downward force of 0.6N on die top surface to mimic spring loading
4. Symmetry boundary conditions in the symmetry plane for 1/4<sup>th</sup> model
5. And fixed support at the end of the tape. Note that model ignores tape's pre-stretch which is expected to have minimal impact

### Model Validation

3D die-pick up simulation also uses the contact debonding cohesive zone modeling approach. In the Figure 17, simulation results at various loading stages has been provided for 4 needle 1mm pitch case which is quarter symmetry model. In the same figure, color contour describes the extent to which tape delamination takes place at each specific needle ejection height. The interface delamination initiation and growth pattern matches the experimental results which is shown in Figure 6. In the Figure 18, ejection height predicted by the model for the successful die-pickup process step is monitored by the contact status where 3 implies no delamination and ~0 implies complete delamination. In the Figure 19, model prediction of successful ejection height has been compared with the experimental data and the model result is in good agreement with the data. This suggest that the FE model with contact debonding approach can be implemented to simulate highly complex loading such as die-pick up event with fairly easily without losing much accuracy.

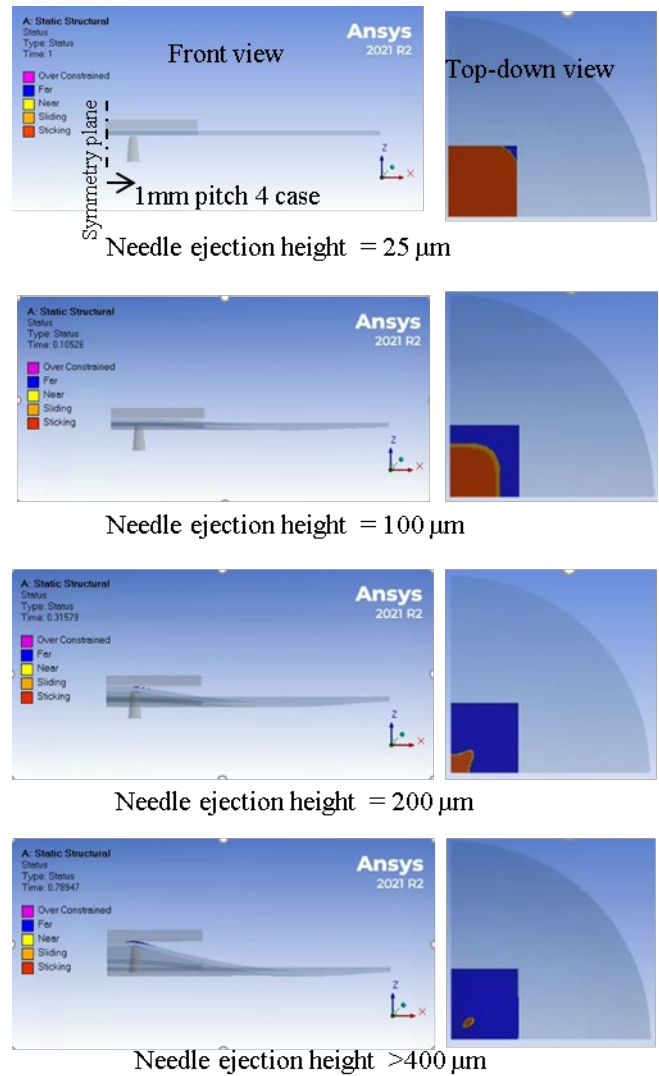


**Figure 17.** Simulation results of tape delamination of die-pickup event at various loading stage for 4 needles 1mm pitch

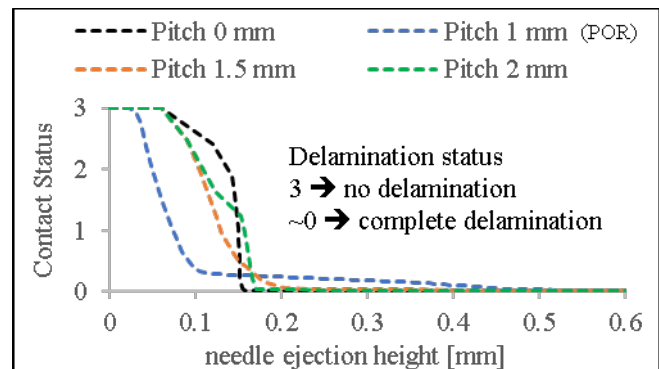


**Figure 18.** Ejection height predicted by the model for the successful die-pickup event

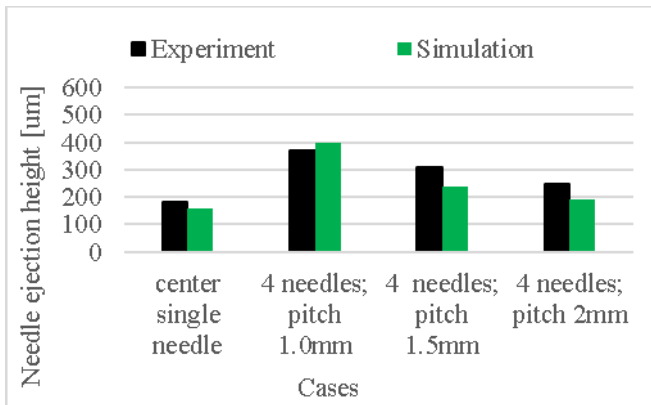


**Figure 19.** comparison of simulated needle ejection height for successful die-pick up w.r.t empirical findings

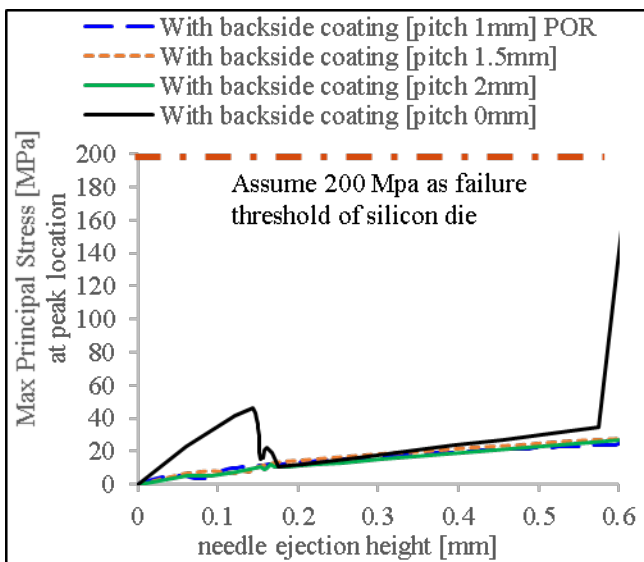


**Figure 20.** Silicon die peak stress during needle ejection event for test cases

In addition to the die-ejection height, model has estimated the stresses in the silicon die during ejection event. The damage metric assumed is the max-principal-stress at the peak location. Figure 20, shows the silicon die stress level for various needle configuration during ejection event. Failure threshold assumed is 200 MPa which is a typical silicon die-strength value on lower side. Based on the simulation results it indicates none-of the case has been subjected to over stress which agree with experimental results where no die has recorded any brittle crack. But in general, process engineer has to be aware of die-pickup process by setting appropriate ejection height level since excess ejection height settings can lead to stress concentration at the bottom surface of die near the needle contact location (see Figure 20, single needle case showing sudden jump in the stress towards end of the 600µm ejection height) and can result in the die brittle crack. Also, lower ejection height settings can result in the unsuccessful die ejection event since dicing tape would continue to stick to the bottom surface of die.

### Die-knocking Risk Evaluation via FE Model

One of the primary failure modes encountered during die-pickup event is the die-knocking issue with adjacent dies. In order to predict die-knocking risk, 2D plane strain model is being implemented to reduce the computation burden. Figure 21 shows the 2D geometry details. Also, in the same figure potential die-knocking region is shown as combination of critical node1 and critical node2.

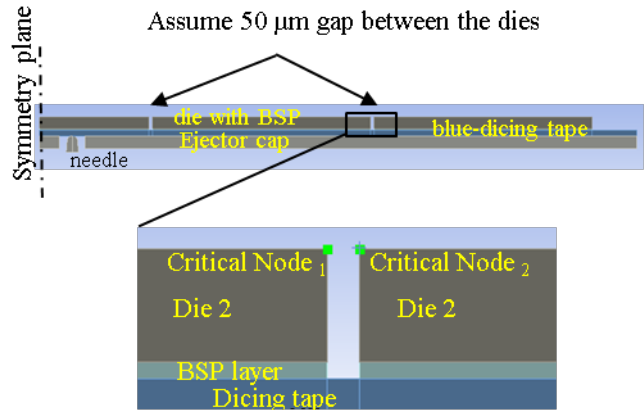


**Figure 21.** Die-knocking risk using 2D plane strain model

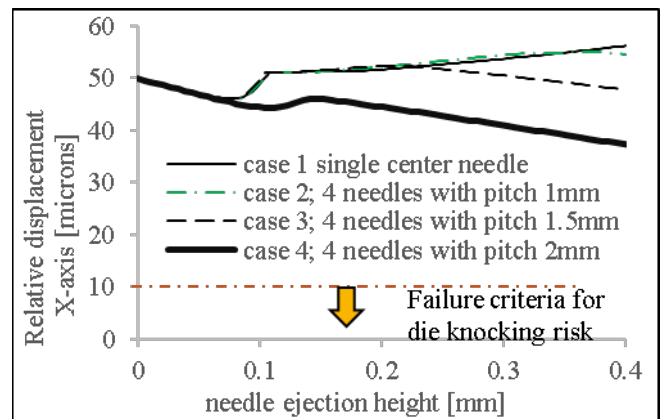


**Figure 22.** Relative displacement between the silicon dies in the critical location during die-pick up event

Figure 22, shows the relative displacement between the silicon dies during the simulated die ejection process step. The failure criteria is set to 10 µm gap between any 2 dies with original gap being 50 µm which is generated during tape pre-stretch. For all the cases simulated, gap between the dies during entire die-pickup event is well above 10 µm indicating the risk of die-knocking for the current set of configuration is minimal. This is in-line with our experiments findings. But in general one has to be aware of the needle misalignment which can trigger the die-knocking issue which is not considered in this study and planned for future studies.

### SUMMARY

WLCSP which is extensively used in the semiconductor industry pose challenges during the electronic assembly. And

one such challenge includes handling thin semi-conductor silicon dies during the die pick up assembly step. The productivity is sensitive to 3 primary factors which include die-crack risk due to ejection process, die knocking to the neighboring dies, unsuccessful die-pickup event. This paper provides step-by-step procedure on how to simulate die-pick up process step using cohesive zone contact debonding fracture mechanics approach. Models have been validated with empirical data in-terms of ejection height, delamination initiation and crack growth path. Modeling result also used to evaluate the potential die crack risk due to over stressing and die-knocking effects. Based on the current study it is recommend to use multiple needle (4+) over single needle for die-ejection to mitigate the die-crack risk. Also, for multi-needle scenario by keeping needle alignment within spec, needles pitch can be set to half of the die size to reduce die-knocking risk and to improve the success rate of the die-ejection event.

## REFERENCES

- [1] B.A., Moris, 'The Science and Technology of Flexible Packaging' Text book. ISBN 978-0-323-24273-8. <https://doi.org/10.1016/C2013-0-00506-3>
- [2] Peng. B., Huang, Y., Yin, Z., Xiong, Y., 'Analysis of interfacial peeling in IC chip pick-up process.' J. Appl. Phys. 110, 073508 (2011); doi: 10.1063/1.3642975
- [3] Liu, Z., Huang, Y., Liu, H., Chen, J., Yin, Z., 'Reliable Peeling of Ultrathin Die with Multineedle Ejector,' IEEE Transactions of component, packaging and manufacturing Technology, vol.4, No.9, September 2014.
- [4] Xu. Z., Liu. Z., Huang, Y., Chen, J., Liu, H., Yin. Z., 'Vaccum-based picking-up of thin chip from adhesive tape,' Article in Journal of Adhesion Science and Technology, March 2015